

21. Detection of the chaotic flow instability in a natural convection loop using the recurrence plot analysis and the nonlinear prediction / Nishikawa H., Matsumura K., Okino S., Watanabe T., Suda F. // Journal of Thermal Science and Technology. 2015. Vol. 10, Issue 2. P. JTST0028–JTST0028. doi: 10.1299/jtst.2015jtst0028
22. Complex network approach for recurrence analysis of time series / Marwan N., Donges J. F., Zou Y., Donner R. V., Kurths J. // Physics Letters A. 2009. Vol. 373, Issue 46. P. 4246–4254. doi: 10.1016/j.physleta.2009.09.042
23. Rusinek R., Zaleski K. Dynamics of thin-walled element milling expressed by recurrence analysis // Meccanica. 2015. Vol. 51, Issue 6. P. 1275–1286. doi: 10.1007/s11012-015-0293-y
24. Recurrence Analysis of Combustion Noise / Kabiraj L., Saurabh A., Nawroth H., Paschereit C. O. // AIAA Journal. 2015. Vol. 53, Issue 5. P. 1199–1210. doi: 10.2514/1.j053285
25. Recurrence plots for the analysis of complex systems / Marwan N., Carmenromano M., Thiel M., Kurths J. // Physics Reports. 2007. Vol. 438, Issue 5-6. P. 237–329. doi: 10.1016/j.physrep.2006.11.001
26. Llop M. F., Gascons N., Llauro F. X. Recurrence plots to characterize gas–solid fluidization regimes // International Journal of Multiphase Flow. 2015. Vol. 73. P. 43–56. doi: 10.1016/j.ijmultiphaseflow.2015.03.003
27. Zbilut J. P., Thomasson N., Webber C. L. Recurrence quantification analysis as a tool for nonlinear exploration of nonstationary cardiac signals // Medical Engineering & Physics. 2002. Vol. 24, Issue 1. P. 53–60. doi: 10.1016/s1350-4533(01)00112-6
28. Examining the learning fire detectors under real conditions of application / Andronov V., Pospelov B., Rybka E., Skliarov S. // Eastern-European Journal of Enterprise Technologies. 2017. Vol. 3, Issue 9 (87). P. 53–59. doi: 10.15587/1729-4061.2017.101985

*Отримано теоретичну та експериментальну оцінки точності неортогональних конфігурацій МЕМС-датчиків на основі як одноосних датчиків, так і триосних вимірювальних блоків. Актуальність дослідження зумовлено можливістю використання таких конфігурацій в навігації безпілотних рухомих об'єктів. Результати було отримано на основі методів інерціальної навігації, аналітичної механіки, математичної статистики та напівнатурного моделювання. Під час досліджень було проаналізовано неортогональні конфігурації одноосних МЕМС-датчиків, включаючи матриці напрямних косинусів. Представлено неортогональні конфігурації на основі інерціальних триосних пристроїв MPU-6050 та конструктивних елементів у вигляді трикутної та чотирикутної пірамід. Отримано відповідні матриці напрямних косинусів. На відміну від відомих неортогональних конфігурацій, враховуються вимірювання усіх датчиків, що входять до складу триосних пристроїв. Надано опис взаємного розташування вимірювальних осей окремих датчиків в запропонованих конфігураціях. Отримано теоретичну оцінку неортогональних конфігурацій МЕМС-датчиків на основі одноосних та триосних вимірювачів кутової швидкості з використанням кореляційних матриць похибок вимірювань. Визначено експериментальну оцінку точності вищезгаданих конфігурацій на підставі динамічного аналізу з використанням триступеневого динамічного стелю просторових переміщень. При цьому надано графічні залежності абсолютних похибок вимірювань та наведено розрахункові значення відносної похибки вимірювання кутової швидкості. Отримані результати є корисними, оскільки вони призначені для забезпечення високоточних та надійних вимірювань, що важливо для безпілотних літальних апаратів, які наразі широко застосовуються в Україні. Результати досліджень можуть також бути застосовані для управління ракетами, що здійснюють запуск малих штучних супутників на орбіту*

*Ключові слова: МЕМС-датчик, неортогональна конфігурація, напрямні косинуси, динамічний аналіз, вимірювальна похибка*

UDC 681.518

DOI: 10.15587/1729-4061.2018.131945

# THEORETICAL AND EXPERIMENTAL ASSESSMENTS OF ACCURACY OF NON- ORTHOGONAL MEMS SENSOR ARRAYS

O. Sushchenko

Doctor of Technical Sciences, Professor\*

E-mail: sushoa@ukr.net

Y. Bezkorovainyi

PhD, Associate Professor\*

E-mail: yurii.bezkor@gmail.com

N. Novytska

Assistant\*

E-mail: n-m@ukr.net

\*Department of Aerospace

Control Systems

National Aviation University

Komarova ave., 1, Kyiv, Ukraine, 03058

## 1. Introduction

Nowadays sensors based on micro-electromechanical systems (MEMS sensors) are widely used in the areas of

navigation and motion control. Among these applications, autopilots of unmanned aerial vehicles (UAVs) and rockets designed for launching small satellites into orbit should be mentioned. These applications are characterized by the high

requirements to accuracy and reliability of measurements. Satisfying these requirements in the case of MEMS sensors usage requires additional research.

Improvement of reliability and accuracy of measurements can be achieved by means of redundancy. It is known that there are possibilities to reserve both the sensors of kinematic parameters (of angular rates, accelerations) and the measuring reference frames. In the first case, the traditional triaxial orthogonal reference frame is used and sensors are located along each of the axis. Under such approach, failure of two sensors can lead to failure of a navigation system as a whole. In the second case, reservation of measuring reference frames is based on the orientation of sensor measuring axes along axes of some geometrical figure.

Applying nonorthogonal redundant configurations for the improvement of reliability and accuracy of measurements has some history [1]. The works [2, 3] contain the detailed description of such configurations [2, 3]. Usage of nonorthogonal redundant configurations of navigational information measuring instruments based on MEMS sensors is characterized by some advantages. In the first place, such configurations provide a decrease of bias. It should be noted that the presence of bias is one of the most important problems of operation of modern MEMS sensors. So, using nonorthogonal redundant configurations improves the accuracy of navigation information measurements. In the second place, the reliability of navigation information is greatly increased due to redundancy. In the third place, such configurations provide the possibility to locate a larger number of sensors in the same dimensions of a constructive unit. This advantage is useful even taking into account miniaturization of modern inertial sensors. The additional advantage is the possibility to increase fault-tolerance of navigation systems.

The topicality of the research in the above-mentioned areas is caused by the necessity to provide the high accuracy and reliability of navigation measurements in motion control systems of unmanned vehicles.

---

## 2. Literature review and problem statement

---

Nowadays the significant attention is paid to the application of nonorthogonal configurations of inertial sensors by reason of development of unmanned aviation. It is marked in modern scientific periodicals that application of redundant fault-tolerant inertial measuring units leads to significant improvement of accuracy and reliability of navigation measurements [4]. Respectively, such configurations can be used for development of inertial navigation systems as shown in [5]. It is expedient to use inertial measuring units based on nonorthogonal configurations in unmanned aviation as grounded in [6]. Nonorthogonal redundant configurations of uniaxial inertial sensors are represented in [7]. The theoretical assessment of accuracy and appropriate comparative analysis of different nonorthogonal configurations is given in [8]. In the above-mentioned papers, nonorthogonal configurations are based on uniaxial sensors [4–6] or on inertial measuring units with the same orientation [7, 8]. Nonorthogonal configurations based on triaxial inertial measuring units with full usage of measuring redundancy require the further research. The problem of navigation accuracy improvement is especially important for control of unmanned vehicles, for example, UAVs, as grounded in [9]. The possibilities to use redundant configurations in fault-tolerance navigation

systems are researched in [10]. Using redundancy of inertial measuring instruments (accelerometers), it is possible even to provide the determination of spatial orientation of a vehicle without application of rate gyroscopes as shown in [11]. It should be noted that sometimes the redundant measuring information arises due to the principle of operation of the navigation measuring instrument. Such a situation takes place in the Coriolis vibratory gyroscope [12]. But usually, it is necessary to form redundant configurations of inertial sensors. The papers [9, 11, 12] confirm the fact of relevance to use redundancy of navigation measurements in motion control systems of unmanned vehicles. The nonorthogonal redundant configuration consisting of triaxial MEMS sensors based on the triangular pyramid is represented in [13]. Approaches to forming such configurations based on both triangular and tetragonal pyramids are given in [14]. So, the research of problems that deal with the assessment of the possibility to use nonorthogonal redundant configurations for navigation applications and to develop more reliable and precise instruments of primary navigation information measurement can be considered promising. Improvement of accuracy of inertial measuring units has both scientific and practical significance due to their wide application in navigation systems of unmanned vehicles.

---

## 3. The aim and objectives of the study

---

The aim of the study is the assessment of accuracy of nonorthogonal redundant configurations based on both single MEMS sensors and triaxial inertial measuring units using triangular and tetragonal pyramids as constructive elements.

To achieve this aim, it is necessary to accomplish the following objectives:

- to analyze configurations of MEMS sensor arrays based on uniaxial inertial measuring instruments;
- to present the results of research of nonorthogonal configurations of MEMS sensor arrays based on triaxial inertial measuring units with the usage of triangular and tetragonal pyramids as construction elements and to determine the tables of directional cosines for the developed nonorthogonal configurations of MEMS sensor arrays;
- to characterize the features of dynamic analysis of a vehicle's angular motion measurement accuracy by means of nonorthogonal redundant inertial measuring instruments from the point of view of the testing equipment and methodical provision;
- to implement theoretical and experimental assessments of nonorthogonal configurations of MEMS sensors arrays, including graphical representation.

---

## 4. Analysis of configurations of MEMS sensor arrays based on uniaxial gyroscopes

---

There are some ways of creation of nonorthogonal configurations based on redundant measuring reference frames [2, 3]:

- 1) use of the cone as a figure of symmetry and orientation of measuring axes of MEMS sensors along the cone's generatrices as shown in Fig. 1, *a*;
- 2) use of the cone as a figure of symmetry and orientation of measuring axes of MEMS sensors along the

cone's generatrices and the axis of symmetry as shown in Fig. 1, *b*;

3) orientation of sensor measuring axes perpendicularly to facets of regular polyhedrons in accordance with Fig. 1, *c, d*.

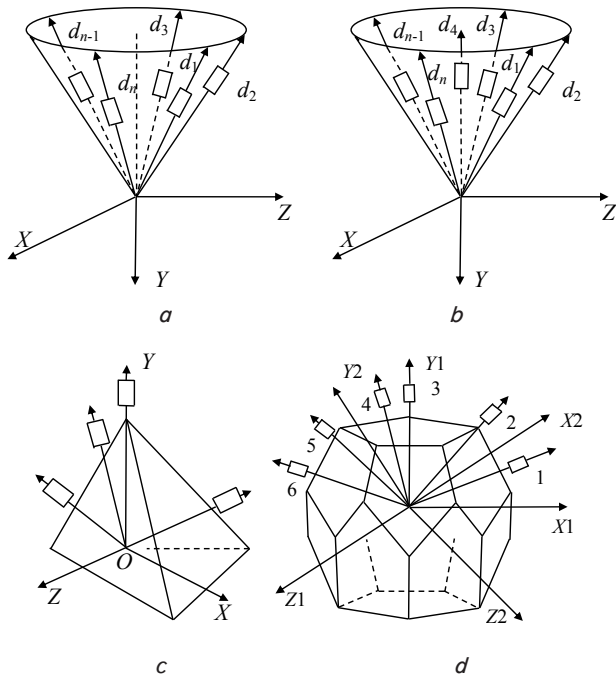


Fig. 1. Nonorthogonal configurations of uniaxial MEMS sensors: *a* – along the cone's generatrices; *b* – along the cone's symmetry axis and generatrices; *c* – perpendicularly to tetrahedron facets; *d* – perpendicularly to dodecahedron facets

One of the basic characteristics of nonorthogonal redundant arrays of inertial sensors is a matrix of directional cosines. Projections of an angular rate of a moving vehicle onto the navigation reference frame can be denoted as  $\omega_x, \omega_y, \omega_z$ . The number of projections of an angular rate onto axes of the measuring reference frame depends on the number of sensors in the configuration. For example, for the configuration consisting of six sensors projections can be denoted as  $d_1, d_2, d_3, d_4, d_5, d_6$ .

Matrices of directional cosines are necessary for transformations of navigation information during the processes of the vehicle's attitude determination. Therefore, the analysis of different configurations of nonorthogonal redundant MEMS sensors arrays must include determination of matrices of directional cosines.

Directional cosines of nonorthogonal redundant arrays of uniaxial MEMS sensors in the case of the orientation of measuring axes of five and six sensors along the cone's generatrices, respectively, are represented in Tables 1, 2. Measuring axes of sensors are tilted relative to the cone's symmetry axis at an angle  $\vartheta$  [2].

If four and five sensors are located along the cone's generatrices and one – along the cone's symmetry axis, directional cosines can be described by Tables 3, 4 [2].

The matrix of directional cosines of the dodecahedron is represented in Table 5. The angle  $\gamma$  between the measuring axes of the sensors is equal to  $31^\circ 43'$  [3].

Table 1

Location of five sensors along the cone's generatrices

Projection	$\omega_x$	$\omega_y$	$\omega_z$
$d_1$	$\sin\vartheta$	$-\cos\vartheta$	0
$d_2$	$-\cos 2\pi / 5 \sin\vartheta$	$-\cos\vartheta$	$\sin 2\pi / 5 \sin\vartheta$
$d_3$	$-\cos \pi / 5 \sin\vartheta$	$-\cos\vartheta$	$\sin 2\pi / 5 \sin\vartheta$
$d_4$	$-\cos \pi / 5 \sin\vartheta$	$-\cos\vartheta$	$-\sin 2\pi / 5 \sin\vartheta$
$d_5$	$\cos 2\pi / 5 \sin\vartheta$	$-\cos\vartheta$	$-\sin 2\pi / 5 \sin\vartheta$

Table 2

Location of six sensors along the cone's generatrices

Projection	$\omega_x$	$\omega_y$	$\omega_z$
$d_1$	$\sin\vartheta$	$-\cos\vartheta$	0
$d_2$	$\cos \pi / 3 \sin\vartheta$	$-\cos\vartheta$	$\sin \pi / 3 \sin\vartheta$
$d_3$	$-\cos \pi / 3 \sin\vartheta$	$-\cos\vartheta$	$\sin \pi / 3 \sin\vartheta$
$d_4$	$\sin\vartheta$	$-\cos\vartheta$	0
$d_5$	$\cos \pi / 3 \sin\vartheta$	$-\cos\vartheta$	$-\sin \pi / 3 \sin\vartheta$
$d_6$	$-\cos \pi / 3 \sin\vartheta$	$-\cos\vartheta$	$-\sin \pi / 3 \sin\vartheta$

Table 3

Location of five sensors

Projection	$\omega_x$	$\omega_y$	$\omega_z$
$d_1$	$-\cos \pi / 4 \sin\vartheta$	$-\cos\vartheta$	$\cos \pi / 4 \sin\vartheta$
$d_2$	$-\cos \pi / 4 \sin\vartheta$	$-\cos\vartheta$	$-\cos \pi / 4 \sin\vartheta$
$d_3$	$\cos \pi / 4 \sin\vartheta$	$-\cos\vartheta$	$-\cos \pi / 4 \sin\vartheta$
$d_4$	$\cos \pi / 4 \sin\vartheta$	$-\cos\vartheta$	$\cos \pi / 4 \sin\vartheta$
$d_5$	0	-1	0

Table 4

Location of six sensors

Projection	$\omega_x$	$\omega_y$	$\omega_z$
$d_1$	$\sin\vartheta$	$-\cos\vartheta$	0
$d_2$	$\cos 2\pi / 5 \sin\vartheta$	$-\cos\vartheta$	$\sin 2\pi / 5 \sin\vartheta$
$d_3$	$-\cos \pi / 5 \sin\vartheta$	$-\cos\vartheta$	$\sin \pi / 5 \sin\vartheta$
$d_4$	$-\cos \pi / 5 \sin\vartheta$	$-\cos\vartheta$	$-\sin \pi / 5 \sin\vartheta$
$d_5$	$\cos 2\pi / 5 \sin\vartheta$	$-\cos\vartheta$	$-\sin 2\pi / 5 \sin\vartheta$
$d_6$	0	-1	0

Table 5

Location of six sensors along dodecahedron facets

Projection	$\omega_x$	$\omega_y$	$\omega_z$
$d_1$	$\cos\gamma$	$-\sin\gamma$	0
$d_2$	$\cos\gamma$	$\sin\gamma$	0
$d_3$	0	$\cos\gamma$	$-\sin\gamma$
$d_4$	0	$\cos\gamma$	$\sin\gamma$
$d_5$	$-\sin\gamma$	0	$\cos\gamma$
$d_6$	$\sin\gamma$	0	$\cos\gamma$

Tables 1–5 can be used for the determination of moving vehicles attitude. Their usage is necessary for navigation information processing.

**5. Features of configurations of MEMS sensor arrays based on inertial measuring units**

Nowadays inertial measuring units, which consist of three MEMS gyroscopes and/or three accelerometers, are widespread in practical applications. Taking this factor into consideration, it is important to create new sensors of orientation and motion based on inertial measuring units rather than single inertial sensors.

Measuring instruments of the considered type are based on sensors with measuring axes oriented perpendicularly to facets of regular polyhedrons [2, 3]. In this case, it is possible to choose such geometrical figure as the tetrahedron (triangular pyramid) and octahedron. From the point of view of construction implementation and dimension restrictions, it is convenient to use half of the octahedron (tetragonal pyramid).

Motion tracking devices MPU-6050 can be used as sensors of primary information in nonorthogonal redundant configurations based on MEMS sensors. The device MPU-6050 (Fig. 2, *a*) has six degrees of freedom and consists of a triaxial gyroscope, triaxial accelerometer, temperature sensor, and also digital motion processor. These units are united in a small package [15]. MPU-6050 includes three 16-bit analog-to-digital converters for digitizing the gyroscope scope outputs and three 16-bit appropriate converters for digitizing the accelerometer outputs. For precision tracking of both fast and slow motions, it is possible to use a user-programmable gyroscope in the measuring range of  $\pm 250$  °/s,  $\pm 500$  °/s,  $\pm 1,000$  °/s,  $\pm 2,000$  °/s, and also a user programmable accelerometer in the measuring range  $\pm 2$  g,  $\pm 4$  g,  $\pm 8$  g,  $\pm 16$  g [15].

The device MPU-6050 and nonorthogonal redundant configuration of MEMS sensors located on facets of the tetragonal pyramid are shown in Fig. 2. Two constructions of the nonorthogonal inertial measuring instruments have been considered. The triangular and tetragonal pyramids are used as constructive elements in these devices. Fig. 2, *b* shows the tetragonal pyramid with inertial measuring units (MPU-6050), which are located on facets, and the microcontroller ATMEGA168, which provides obtaining and processing of navigation information. The measuring instrument is mounted at the test bench.

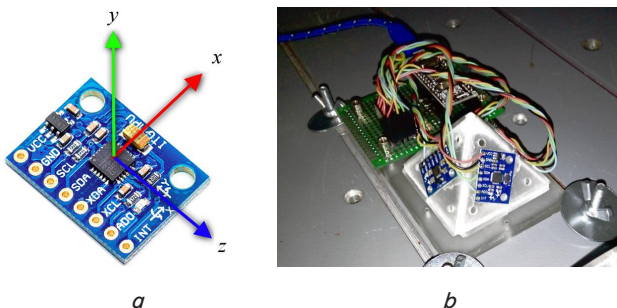


Fig. 2. The nonorthogonal configuration of MEMS sensors: *a* – the device MPU-6050; *b* – the inertial measuring unit with the usage of the tetragonal pyramid as a constructive element

The represented configuration of MEMS sensor arrays can be used in systems that provide navigation of unmanned vehicles, for example, unmanned aerial vehicles or rockets for launching small low-cost satellites into orbit.

**6. Matrices of directional cosines of nonorthogonal redundant configurations of MEMS sensor arrays**

To obtain navigation information using nonorthogonal inertial measuring instruments, it is necessary to determine the navigation reference frame *xyz* and appropriate measuring reference frames. Usually, axes of the navigation reference frame connected with an aircraft are determined in the following way: the longitudinal (*x*), normal (*y*) and lateral (*z*) axes, respectively. The axis *y* is up-directed along the pyramid symmetry axis. Axes *x*, *z* of the navigation reference frame coincide with appropriate axes of the inertial measuring unit located at the pyramid base.

Directions of measuring axes are opposite to increase the reliability of navigation information. Directions of axes are chosen to make angles between them as large as possible. This leads to decreasing bias influence during the determination of angular rate projections onto axes of the navigation reference frame. Mutual location of axes of measuring reference frames of separate inertial measuring units for such constructive element as the triangular pyramid is represented in Fig. 3.

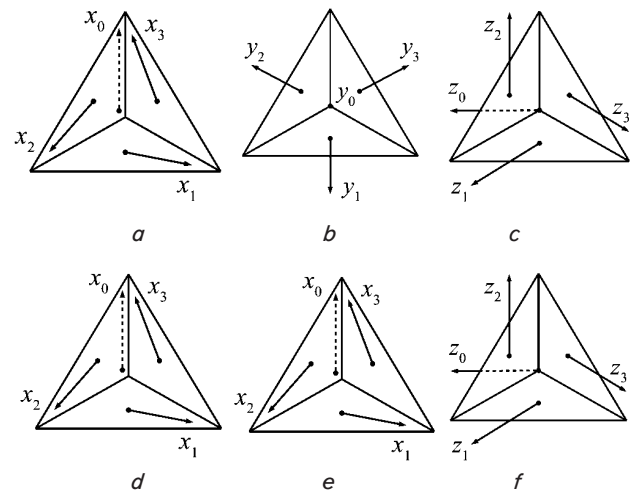


Fig. 3. Location of axes of measuring reference frames on facets of the triangular pyramid: *a* – the frontal view of the axes  $x_0, x_1, x_2, x_3$ ; *b* – the frontal view of the axes  $y_0, y_1, y_2, y_3$ ; *c* – the frontal view of the axes  $z_0, z_1, z_2, z_3$ ; *d* – the top view of the axes  $x_0, x_1, x_2, x_3$ ; *e* – the top view of the axes  $y_0, y_1, y_2, y_3$ ; *f* – the top view of the axes  $z_0, z_1, z_2, z_3$

There are two ways to determine matrices of directional cosines. The first way is obtaining projections of the unit vector using geometrical transformations. The second way is determination of directional cosines between the navigation reference frame and measuring reference frames by means of successive turns at some definite angles. The first approach requires fewer transformations and calculations, respectively. The advantage of the second way is clearness. An additional complication of calculations of the second approach can be compensated by the possibility to automate calculations by means of MatLab.

Using the basic laws of the analytic mechanics [16], the expressions for determination of directional cosines of the nonorthogonal configuration based on such a construction unit as the triangular pyramid can be represented in the following form

$$\begin{aligned}
 \mathbf{D}_1 &= \mathbf{A}_x; \\
 \mathbf{D}_2 &= \mathbf{A}_{y1}\mathbf{A}_z\mathbf{A}_y; \\
 \mathbf{D}_3 &= \mathbf{A}_{y2}\mathbf{A}_z\mathbf{A}_y; \\
 \mathbf{D}_4 &= \mathbf{A}_{y3}\mathbf{A}_z\mathbf{A}_y,
 \end{aligned}
 \tag{1}$$

where  $\mathbf{D}_1, \mathbf{D}_2, \mathbf{D}_3, \mathbf{D}_4$  are block matrices of directional cosines between axes of the navigation reference frame and reference frames of the inertial measuring units. The matrix  $\mathbf{A}_x$  defines axes of the inertial measuring unit based on the triangular pyramid. The matrix  $\mathbf{A}_y$  characterizes a slope of measuring axes of inertial measuring units based on the pyramid facets relative to the horizontal plane. Matrices  $\mathbf{A}_{y1}, \mathbf{A}_{y2}, \mathbf{A}_{y3}$  define the location of axes of inertial measuring units relative to the previous axes. The matrix  $\mathbf{A}_z$  defines axes of inertial measuring units located on lateral facets along their medians at the angle  $120^\circ$ . For the triangular pyramid, the angle between the base and the lateral facet is equal to  $70.5^\circ$ . Matrices that are components of the expression (1) can be represented in the following form

$$\begin{aligned}
 \mathbf{A}_x &= \begin{bmatrix} 1 & 0 & 0 \\ 0 & \cos \gamma & \sin \gamma \\ 0 & -\sin \gamma & \cos \gamma \end{bmatrix}; \\
 \mathbf{A}_y &= \begin{bmatrix} \cos \psi_0 & 0 & -\sin \psi_0 \\ 0 & 1 & 0 \\ \sin \psi_0 & 0 & \cos \psi_0 \end{bmatrix}; \\
 \mathbf{A}_{y_i} &= \begin{bmatrix} \cos \psi_i & 0 & -\sin \psi_i \\ 0 & 1 & 0 \\ \sin \psi_i & 0 & \cos \psi_i \end{bmatrix}; \\
 \mathbf{A}_z &= \begin{bmatrix} \cos \vartheta & -\sin \vartheta & 0 \\ \sin \vartheta & \cos \vartheta & 0 \\ 0 & 0 & 1 \end{bmatrix},
 \end{aligned}
 \tag{2}$$

where  $i=1,2,3; \gamma=180^\circ; \psi_0=120^\circ; \psi_1=0^\circ; \psi_2=120^\circ; \psi_3=240^\circ; \vartheta=70,5^\circ; \gamma$  is determined for the base of the pyramid;  $\psi_i$  determine angles of turn of lateral facets;  $\psi_0$  determines a turn relative to axes that are normal to the facets;  $\vartheta$  is the angle of the facet slope.

Substituting matrices (2) in the expression (1), it is possible to determine the mutual location of navigation and measuring reference frames. Finally, the table of directional cosines between the navigation reference frame and measuring reference frames of inertial units located on facets of the triangular pyramid is represented in Table 6.

Location of axes of measuring reference frames of separate inertial measuring units for such a constructive unit as a tetragonal pyramid is represented in Fig. 4.

Directional cosines of the nonorthogonal redundant configuration based on the tetragonal pyramid can be determined in a similar way taking into consideration a slope between the base and the side facet, which is equal to  $54.74^\circ$ .

Table 6

Table of directional cosines for the configuration using the triangular pyramid as a constructive unit

Projection	$\omega_x$	$\omega_y$	$\omega_z$
$d_1 = \omega_x^1$	1	0	0
$d_2 = \omega_y^1$	0	$\cos \gamma$	$-\sin \gamma$
$d_3 = \omega_z^1$	0	$\sin \gamma$	$\cos \gamma$
$d_4 = \omega_x^2$	$-\sin \psi_0 \sin \psi_1 + \cos \psi_0 \cos \psi_1 \cos \vartheta$	$-\sin \vartheta \cos \psi_1$	$\sin \psi_0 \cos \psi_1 \cos \vartheta + \sin \psi_1 \cos \psi_0$
$d_5 = \omega_y^2$	$\sin \vartheta \cos \psi_0$	$\cos \vartheta$	$\sin \psi_0 \sin \vartheta$
$d_6 = \omega_z^2$	$-\sin \psi_0 \cos \psi_1 - \sin \psi_1 \cos \psi_0 \cos \vartheta$	$-\sin \gamma$	$-\sin \psi_0 \sin \psi_1 \cos \vartheta + \cos \psi_0 \cos \psi_1$
$d_7 = \omega_x^3$	$-\sin \psi_0 \sin \psi_2 + \cos \psi_0 \cos \psi_2 \cos \vartheta$	$\cos \gamma$	$\sin \psi_0 \cos \psi_2 \cos \vartheta + \sin \psi_2 \cos \psi_0$
$d_8 = \omega_y^3$	$\sin \vartheta \cos \psi_0$	$\cos \vartheta$	$\sin \psi_0 \sin \vartheta$
$d_9 = \omega_z^3$	$-\sin \psi_0 \cos \psi_2 - \sin \psi_2 \cos \psi_0 \cos \vartheta$	$\sin \psi_2 \sin \vartheta$	$-\sin \psi_0 \sin \psi_2 \cos \vartheta + \cos \psi_0 \cos \psi_2$
$d_{10} = \omega_x^4$	$-\sin \psi_0 \sin \psi_3 + \cos \psi_0 \cos \psi_3 \cos \vartheta$	$-\sin \vartheta \cos \psi_3$	$\sin \psi_0 \cos \psi_3 \cos \vartheta + \sin \psi_3 \cos \psi_0$
$d_{11} = \omega_y^4$	$\sin \vartheta \cos \psi_0$	$\cos \vartheta$	$\sin \psi_0 \sin \vartheta$
$d_{12} = \omega_z^4$	$-\sin \psi_0 \cos \psi_3 - \sin \psi_3 \cos \psi_0 \cos \vartheta$	$\sin \psi_3 \sin \vartheta$	$-\sin \psi_0 \sin \psi_3 \cos \vartheta + \cos \psi_0 \cos \psi_3$

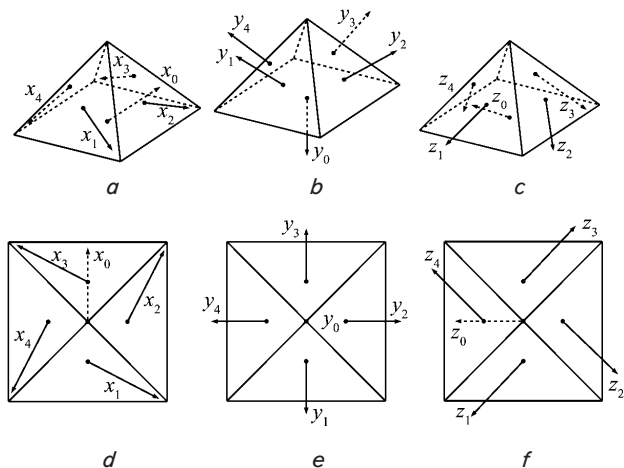


Fig. 4. Location of axes of measuring reference frames on facets of the tetragonal pyramid: a – the frontal view of the axes  $x_0, x_1, x_2, x_3, x_4$ ; b – the frontal view of the axes  $y_0, y_1, y_2, y_3, y_4$ ; c – the frontal view of the axes  $z_0, z_1, z_2, z_3, z_4$ ; d – the top view of the axes  $x_0, x_1, x_2, x_3, x_4$ ; e – the top view of the axes  $y_0, y_1, y_2, y_3, y_4$ ; f – the top view of the axes  $z_0, z_1, z_2, z_3, z_4$

Directional cosines of the nonorthogonal redundant configuration based on such a constructive unit as tetragonal pyramid can be represented in the following form

$$D_1 = A_x; D_2 = A_{y1}A_zA_y; D_3 = A_{y2}A_zA_y;$$

$$D_4 = A_{y3}A_zA_y; D_5 = A_{y4}A_zA_y.$$

The matrix  $A_x$  defines the orientation of axes of the inertial measuring units located on the base of the tetragonal pyramid. The angle  $\vartheta$  is equal to  $54.74^\circ$ . It determines the slope of the lateral facet to the base of the tetragonal pyramid. Angles  $\psi_i$  define the orientation of axes of measuring frames of units located on the lateral facets. They are equal to  $0^\circ, 90^\circ, 180^\circ, 270^\circ$ , respectively.

The table of directional cosines (numerical data) for the nonorthogonal redundant configuration, which uses the tetragonal pyramid as a constructive element, is represented in Table 7.

Table 7

Table of directional cosines (tetragonal pyramid)

Projection	$\omega_x$	$\omega_y$	$\omega_z$
$d_1 = \omega_x^1$	1	0	0
$d_2 = \omega_y^1$	0	-1	0
$d_3 = \omega_z^1$	0	0	-1
$d_4 = \omega_x^2$	-0.28868	-0.81650	-0.50000
$d_5 = \omega_y^2$	-0.40825	0.57735	-0.70711
$d_6 = \omega_z^2$	0.86603	0	0.5
$d_7 = \omega_x^3$	0.86603	0	0.5
$d_8 = \omega_y^3$	-0.40825	0.57735	-0.70711
$d_9 = \omega_z^3$	0.28868	0.81650	0.5
$d_{10} = \omega_x^4$	0.86603	0	0.5
$d_{11} = \omega_y^4$	-0.40825	0.57735	-0.70711
$d_{12} = \omega_z^4$	0.28868	0.81650	0.5
$d_{13} = \omega_x^5$	-0.86603	0	0.5
$d_{14} = \omega_y^5$	-0.40825	0.57735	-0.70711
$d_{15} = \omega_z^5$	-0.28868	-0.81650	-0.5

It should be noted that expressions for direction cosines determination are simpler in comparison with the configuration using the constructive unit based on the triangular pyramid.

**7. Features of dynamic analysis of accuracy of inertial measuring units**

In contrast to the static analysis, the dynamic analysis allows estimating the accuracy of the inertial measuring instrument in conditions of spatial angular motions by means of the three-degree-of-freedom test bench, which is represented in Fig. 5.

The principle of operation of the test bench is as follows. The testing inertial measuring instrument is mounted on the test bench platform in a position, which corresponds to the location of the inertial measuring instrument during the operation of the inertial measuring instrument on a vehicle. Simulation of the tested instrument dynamics is implemented by means of software. The software provides the simula-

tion of angular motion around axes of the reference frame of the test bench. Axes of the test bench reference frame coincide with axes of the navigation reference frame.



Fig. 5. The three-degree-of-freedom dynamic test bench

The dynamic three-degree-of-freedom bench consists of the power plant, computer, control unit, three step-motors, three angle sensors, and platform, which is mounted in gimbals. The structural scheme of the dynamic test bench is shown in Fig. 6, a. Readings of motion tracking devices MPU-6050 are taken by means of the microcontroller ATMEGA168. The scheme of connection of the motion tracking device and the microcontroller is represented in Fig. 6, b.

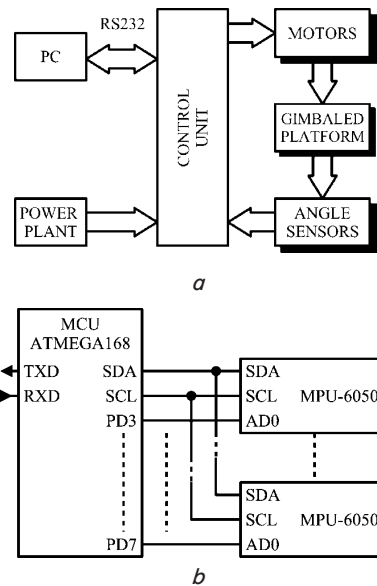


Fig. 6. Facilities of dynamic analysis (PC – personal computer): a – structural scheme of the dynamic bench; b – scheme of connection of the inertial measuring unit and the microcontroller

Recording and processing of navigation information are implemented by specially developed software. The software provides a synchronous reading of information about angular rates, which enters from separate MEMS gyroscopes. The software consists of the console utility installed in the computer, and the microcontroller ATMEGA168 software.

The information exchange is implemented by means of the serial interface UART. The arithmetic and logic unit of the microcontroller ATMEGA168 does not support floating point operations. Moreover, accuracy and processing power of these operations in the compatibility mode are very low. Therefore, it is convenient to carry out basic calculations by means of the computer.

The efficiency of angular motion simulation can be increased by simulation of errors caused by random external disturbances. In the general case, the dynamic test bench gives the wide possibilities for simulation of deterministic and stochastic angular motion. Control of the dynamic test bench is automated. The change of simulated motion parameters is implemented by means of interface windows, which appear on the computer display.

The nonorthogonal inertial measuring instrument is located on the platform of the three-degree-of-freedom test bench. The platform of the test bench is mounted in gimbals. This provides the possibility of simulation of arbitrary angular motions relative to three axes, which correspond to axes of the navigation reference frame. Simulation of motions relative to each of the navigation reference frame axis is carried out by means of testing signals, which represent harmonic signals with different periods. These signals can be represented in the following form

$$\begin{aligned}
 x(t) &= 5\sin(\pi/6 \cdot t); \\
 y(t) &= 5\sin(\pi/12 \cdot t); \quad z(t) = 5\sin(\pi/4 \cdot t). \quad (3)
 \end{aligned}$$

It is known that MEMS gyroscopes are characterized by errors due to zero bias caused by the influence of temperature and initial bias. Compensation of the above-listed factors can be implemented in the following way. In the first place, the nonorthogonal inertial measuring instrument must function in the mode of no-load operation during 15...20 min. This is carried out for temperature stabilization of MEMS sensors and compensation of the zero drift. The platform is immovable in this mode. In the second place, the residual bias is estimated during 1 min. This allows determining the systematic error  $\Delta_r$ . After these procedures, the angular motion of the test bench is given in the program way. Angular motions (3) act during 5 min after temperature stabilization. This process coincides with the beginning of measuring information recording. The experiment is accompanied by a synchronous recording of both information about the angular position of the test bench and information measured by MEMS sensors with the frequency of 100 Hz.

**8. Discussion of results of theoretical and experimental assessments of nonorthogonal redundant configurations based on MEMS sensor arrays**

*Theoretical assessment.* Using the nonorthogonal redundant MEMS sensor arrays requires conversion of measuring information, which is determined in the nonorthogonal reference frame, into information in the orthogonal (body-axis) reference frame. Such a conversion can be described by the matrix of the directional cosines **H**.

The least square method can be used for processing of redundant information [2, 3]. The minimum trace of the correlation matrix of errors can be chosen as the optimization criterion for this method. In this case, the statistic charac-

teristics of the measuring parameter are believed to be independent and the mathematical expectation – equal to zero. If these assumptions are satisfied, the correlation matrix of errors can be determined by the expression [3]

$$\mathbf{D} = [\mathbf{H}^T \mathbf{H}]^{-1}. \quad (4)$$

The matrix trace **D** is the sum of the diagonal elements, which are variances of measuring errors [3]

$$tr(\mathbf{D}) = \sum_{i=1}^n d_{ii}, \quad (5)$$

where  $d_{ii}$  are the diagonal elements of the matrix **D**;  $n$  is the number of sensors.

Comparative analysis of accuracy of different types of nonorthogonal redundant configurations of inertial measuring units can be done on the basis of the expressions (4), (5) in correspondence with [2, 3]. For example, if the nonorthogonal configuration consists of six sensors located on the cone's generatrices, the matrix **H** is described in Table 2. In this case, the correlation matrix of errors can be determined in the following way

$$tr[\mathbf{H}^T \mathbf{H}]^{-1} = tr \begin{bmatrix} 0.5 & 0 & 0 \\ 0 & 0.5 & 0 \\ 0 & 0 & 0.5 \end{bmatrix} = 1.5.$$

The results of the comparative analysis of accuracy for different nonorthogonal configurations of uniaxial sensors according to the formulas (5), (6) are represented in Table 8. This table includes data about values of traces of the correlation matrices of errors for different nonorthogonal redundant configurations in different situations of sensor failures.

Table 8

Results of comparative analysis of nonorthogonal configurations of uniaxial inertial sensors

Type of configuration	Trace of correlation matrix of errors		
	Without failures	Failures of 2 sensors	Failures of 3 sensors
5 sensors along the cone's generatrices	2.21	3.20	3.92
6 sensors along the cone's generatrices	1.79	2.13	4.50
4 sensors along the cone's generatrices and 1 along the symmetry axis	1.93	3.15	5.00
5 sensors along the cone's generatrices and 1 along the symmetry axis	1.70	2.18	3.35
6 sensors perpendicular to facets of the dodecahedron	1.50	2.00	3.00

Comparative analysis of accuracy of nonorthogonal measuring instruments based on inertial measuring units is represented in Table 9.

The results represented in Table 9 prove advantages on the accuracy of the nonorthogonal redundant configuration using the tetragonal pyramid.

Table 9

Results of comparative analysis of nonorthogonal configurations based on inertial measuring units

Type of configuration	Trace of correlation matrix of errors
Orthogonal configuration	1.0
Configuration using the triangular pyramid	0.75
Configuration using the tetragonal pyramid	0.6

*Experimental assessment.* Recorded information includes data about the vector of the space attitude of the platform

$$\phi = [\psi \ \vartheta \ \gamma]^T, \tag{6}$$

where angles  $\psi$ ,  $\vartheta$ ,  $\gamma$  correspond to the rotation of the platform in the horizontal, vertical, and lateral planes, respectively. The vector of the measured angular rate of the platform on projections onto axes of the navigation reference frame is determined in the following way

$$\Omega = [\omega_x^1 \ \omega_y^2 \ \omega_z^3 \ \dots \ \omega_x^{n-2} \ \omega_y^{n-1} \ \omega_z^n]^T, \tag{7}$$

where  $n$  is the number of MEMS sensors ( $3 \times 4$  for the non-orthogonal measuring instrument based on the constructive unit in the form of the triangular pyramid and  $3 \times 5$  – for the tetragonal pyramid, respectively). The vector of the measured angular rate of the test bench in projections of the navigation reference frame based on the expressions (6) and (7) can be determined in the following way

$$\omega_\phi^T = [\omega_\psi \ \omega_\vartheta \ \omega_\gamma] = \Omega^T \mathbf{H}. \tag{8}$$

Further averaging of the measured angular rate (8) is carried out

$$\omega_{\phi \text{ av}} = \frac{1}{m} \sum_{i=1}^m \omega_{\phi_i}, \quad \phi = \psi, \vartheta, \gamma, \tag{9}$$

where  $m$  is the number of measurements.

The assessment of accuracy of the inertial measuring instrument can be determined by comparison of the measured angular rate (9) and the given angular rate of the test bench (6). It is necessary also to take into consideration the systematic temperature error

$$\varepsilon_\phi = \omega_{\phi \text{ av}} - \phi' - \Delta_{t\phi}, \quad \phi = \psi, \vartheta, \gamma, \tag{10}$$

where  $\varepsilon_\phi$  is the measuring error of the inertial measuring unit,  $\phi'$  is the derivative of the given angular position of the test bench.

It is known that the root mean square (RMS) is the most widespread representation of the measuring error. Respectively, the relationship for determination of the variance taking into consideration the expression (10) becomes

$$\sigma_\phi = \sqrt{\frac{1}{m-1} \sum_{i=1}^m (\varepsilon_{\phi_i} - \varepsilon_\phi)^2}, \quad \phi = \psi, \vartheta, \gamma; \quad i = 1, \dots, m.$$

The dynamic analysis has been carried out using the three-degree-of-freedom test bench and the above-stated

technique of the RMS error determination. It should be noted that during the experiment the estimated angular rate has been given in one direction only.

At first, the assessment of accuracy of the single motion tracking device MPU-6050 was carried out. The results of this experiment are represented in Fig. 7, which shows projections of the measured angular rate onto axes of the navigational reference frame. Such an approach has been chosen for the possibility to compare errors of measurements of the single measuring unit and redundant navigation measuring instruments using such constructive units as triangular and tetragonal pyramids.

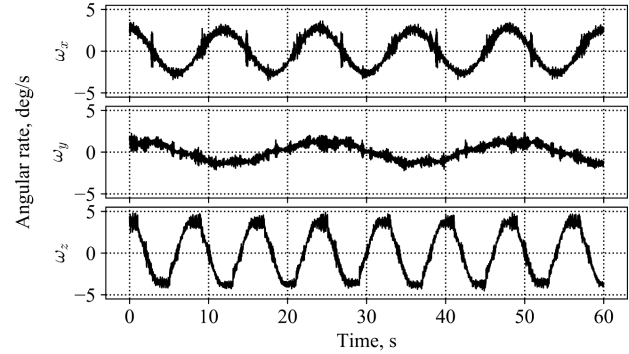


Fig. 7. Graphical dependences of angular rates

The results of the dynamic analysis of nonorthogonal redundant inertial measuring instruments based on such constructive elements as triangular and tetragonal pyramids are represented in Fig. 8. These data are averaging of the readings of angular rates measured in correspondence with the above-represented technique. The obtained results of measurements were converted into projections of angular rates onto axes of the navigation reference frame according to matrices of directional cosines represented in Tables 6, 7.

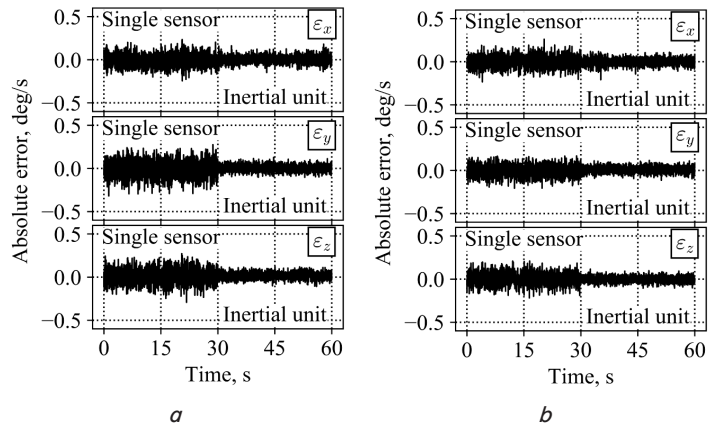


Fig. 8. The absolute error of determination of the vehicle angular rate by means of the nonorthogonal redundant inertial measuring instrument: *a* – on the basis of the triangular pyramid; *b* – on the basis of the tetragonal pyramid

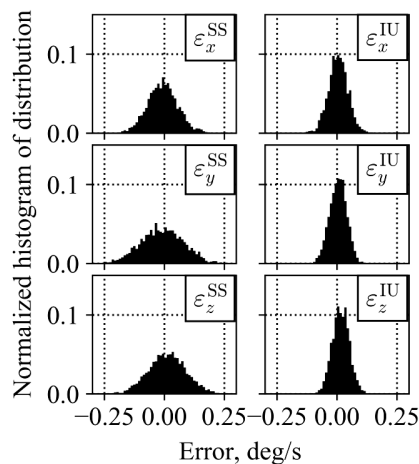
Comparison of measuring the accuracy of different nonorthogonal redundant measuring instruments shows that the usage of measuring instruments on the basis of the tetragonal pyramid is more effective from the point of view of accuracy improvement.

Histograms of distribution of absolute errors of measurement of angular rates relative to axes of the navigation reference frame are represented in Fig. 9. Analysis of these histograms shows that random errors of determination of motion parameters are distributed by the normal law. The experimental assessment of accuracy (Table 10) has been carried out on the basis of a ratio of the normalized value of the RMS error of the nonorthogonal inertial measuring instrument to the RMS error of the single MEMS sensor.

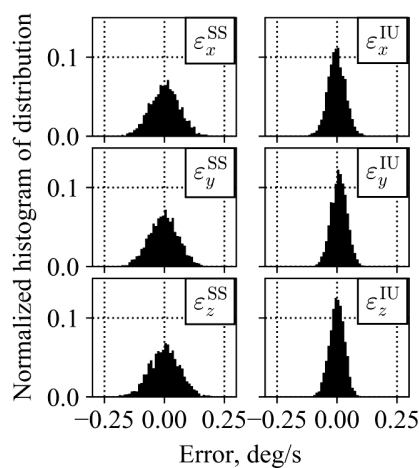
Table 10

Results of the experimental assessment of RMS errors of measurement of angular rate projections

Type of constructive unit	$\sigma_{rel} = \sigma_i / \sigma_i^0$		
	<i>x</i>	<i>y</i>	<i>z</i>
Triangular pyramid	0.6651	0.5094	0.4845
Tetragonal pyramid	0.5481	0.4163	0.4460



a



b

Fig. 9. Histograms of distribution of errors for the nonorthogonal redundant measuring instrument (SS – single sensor, IU – inertial unit): a – on the basis of the triangular pyramid; b – on the basis of the tetragonal pyramid

Table 10 includes information about normalized values of RMS errors of measured projections of the moving base (test bench) angular rates projections in the navigation reference frame by means of different types of nonorthogonal redundant inertial measuring instruments. Normalization is carried relative to the RMS of the orthogonal triaxial inertial sensor. In accordance with Table 10, the nonorthogonal redundant measuring instrument based on such a constructive unit as the tetragonal pyramid provides the higher accuracy in comparison with the measuring instrument based on the triangular pyramid for all axes of the navigation reference frame.

The advantage of the research is the creation of nonorthogonal configurations based on triaxial inertial measuring units. This has practical significance as inertial MEMS sensors of this type are used in the modern applied navigation. At the following stages, tests of the researched nonorthogonal redundant measuring instrument as a part of UAV autopilot should be carried out. The results of the research will be useful for the area of navigation using measuring instruments based on MEMS sensors. It is expedient to use these instruments in motion control systems of unmanned vehicles. Direct practical use of the developed configurations of nonorthogonal measuring instruments is bounded due to two factors. In the first place, there are rather significant errors during manufacturing of prototypes. In the second place, zero drift of single MEMS sensors during the change of operating temperature conditions worsens accuracy. The presented result is only part of the research, which covers a number of problems connected with the design of nonorthogonal configurations of triaxial MEMS sensors. Development of calibration technique of the nonorthogonal configuration based on the learning algorithm is planned in the future.

### 9. Conclusions

1. Analysis of nonorthogonal configurations based on uniaxial MEMS sensors is carried out. The appropriate matrices of directional cosines obtained on the basis of relationships of analytical mechanics are represented. Also matrices of directional cosines, which provide conversion of measuring information into navigation one are given. These matrices were developed for nonorthogonal configurations with maximum usage of redundancy due to different orientation of inertial triaxial sensors located on facets of the triangular and tetragonal pyramids.
2. The procedure of the dynamic analysis of accuracy of nonorthogonal redundant inertial instruments of vehicle angular rate measurement is proposed. Features of the procedure are the simulation of the vehicle angular motion in the inertial space by means of the three-dimensional dynamic test bench and determination of assessments of random measuring errors based on the experimental data.
3. Experimental samples of nonorthogonal configurations based on triaxial inertial device MPU-60 and construction elements in the form of triangular and tetragonal pyramids are developed and researched.
4. Comparative theoretical assessment of accuracy of nonorthogonal configurations based on uniaxial and triaxial MEMS sensors with the usage of correlation matrices of errors had shown advantages of the proposed measuring instruments. For example, configurations based on the tetrag-

onal pyramid for uniaxial sensors and triaxial inertial units for measurement of angular rates are characterized by the error based on the trace of the correlation matrix 1.93 and 0.6, respectively, for the case without failures. This result is also proved by the presented graphical dependences based on the experimental data. The results of dynamic analysis

have been shown advantages of the construction based on the tetragonal pyramid. In this case, normalized values of measuring RMS error along all measuring axes are less than appropriate errors for the configuration based on the triangular pyramid (0.55; 0.42; 0.43 and 0.67; 0.51; 0.49, respectively).

## References

1. Pejsa A. J. Optimum Skewed Redundant Inertial Navigators // *AIAA Journal*. 1974. Vol. 12, Issue 7. P. 899–902. doi: 10.2514/3.49378
2. Epifanov A. D. *Nadezhnost' sistem upravleniya*. Moscow: Mashinostroenie, 1975. 144 p.
3. Epifanov A. D. *Izbytochnye sistemy upravleniya letatel'nyimi apparatami*. Moscow: Mashinostroenie, 1978. 178 p.
4. Dai X., Zhao L., Shi Z. Fault Tolerant Control in Redundant Inertial Navigation System // *Mathematical Problems in Engineering*. 2013. Vol. 2013. P. 1–11. doi: 10.1155/2013/782617
5. Redundant MEMS-Based Inertial Navigation Using Nonlinear Observers / Rogne R. H., Bryne T. H., Fossen T. I., Johansen T. A. // *Journal of Dynamic Systems, Measurement, and Control*. 2018. Vol. 140, Issue 7. P. 071001. doi: 10.1115/1.4038647
6. Song J. W., Park C. G. Optimal Configuration of Redundant Inertial Sensors Considering Lever Arm Effect // *IEEE Sensors Journal*. 2016. Vol. 16, Issue 9. P. 3171–3180. doi: 10.1109/jsen.2015.2510545
7. Jafari M. Optimal redundant sensor configuration for accuracy increasing in space inertial navigation system // *Aerospace Science and Technology*. 2015. Vol. 47. P. 467–472. doi: 10.1016/j.ast.2015.09.017
8. Jafari M., Roshanian J. Optimal Redundant Sensor Configuration for Accuracy and Reliability Increasing in Space Inertial Navigation Systems // *Journal of Navigation*. 2012. Vol. 66, Issue 02. P. 199–208. doi: 10.1017/s0373463312000434
9. Sushchenko O. A., Golitsyn V. O. Data processing system for altitude navigation sensor // 2016 4th International Conference on Methods and Systems of Navigation and Motion Control (MSNMC). 2016. doi: 10.1109/msnmc.2016.7783112
10. Larin V. B., Tunik A. A. Fault-tolerant strap-down inertial navigation systems with external corrections // *Applied and Computational Mathematics*. 2015. Vol. 14, Issue 1. P. 23–37.
11. Larin V. B., Tunik A. A. On Inertial-Navigation System without Angular-Rate Sensors // *International Applied Mechanics*. 2013. Vol. 49, Issue 4. P. 488–499. doi: 10.1007/s10778-013-0582-x
12. Chikovani V., Sushchenko O., Tsiruk H. Redundant information processing techniques comparison for differential vibratory gyroscope // *Eastern-European Journal of Enterprise Technologies*. 2016. Vol. 4, Issue 7 (82). P. 45–52. doi: 10.15587/1729-4061.2016.75206
13. Parshin A. P., Nemshilov Y. A. Development of measurement UAV attitude control unit with non-orthogonal arrangement of sensing elements // *Modern technics and technologies*. 2016. Issue 3. URL: <http://technology.snauka.ru/2016/03/9697>
14. Sushchenko O. A., Bezkorovainyi Y. N., Novytska N. D. Nonorthogonal redundant configurations of inertial sensors // 2017 IEEE 4th International Conference Actual Problems of Unmanned Aerial Vehicles Developments (APUAVD). 2017. doi: 10.1109/apuavd.2017.8308780
15. MPU-6000 and MPU-6050 Product Specification. URL: [https://store.invensense.com/datasheets/invensense/MPU-6050\\_Data-Sheet\\_.pdf](https://store.invensense.com/datasheets/invensense/MPU-6050_Data-Sheet_.pdf)
16. Lurie A. I. *Analytical mechanics*. Springer, 2002. 864 p. doi: 10.1007/978-3-540-45677-3